Geophysical model of the lithosphere across the Variscan Belt of SW-Iberia: Multidisciplinary assessment

I. Palomeras [a,*], R. Carbonell [a], P. Ayarza [b], M. Fernàndez [a], J.F. Simancas [c], D. Martínez Poyatos [c], F. González Lodeiro [c], A. Pérez-Estaún [a]

[a] Departamento de Estructura y Dinámica de la Tierra, CSIC-Instuituto de Ciencias de la Tierra Jaume Almera, c/Lluís Solé i Sabarís s/n, 08028 Barcelona, Spain
[b] Departamento de Geología, Universidad de Salamanca, Pl de la Merced s/n, 37008 Salamanca, Spain
[c] Departamento de Geodinámica, Universidad de Granada, Av. Fuentenueva s/n, Granada 19071, Spain

ARTICLE INFO

ABSTRACT

A multidisciplinary geophysical study along a large seismic transect in the SW-Iberian Peninsula has been carried out. This study integrates the crustal structure, geometry and composition obtained from normal incidence and wide-angle seismic reflection data with other observables (geoid, gravity and topography). The internal architecture of the lithosphere across the Variscan Orogen of SW-Iberia is constrained by the 300 km long high resolution deep normal seismic reflection IBERSEIS Transect. The most prominent feature imaged by the seismic survey is the Iberseis Reflective Body (IRB), a 140 km long high amplitude reflective body located in the middle crust of the northern half of the transect. The seismic velocity (Vp) distribution within the crust and the upper mantle is constrained by two wide-angle seismic transects acquired in the same area. The velocity models show a complex crust, with a specially complex middle crust, which features higher velocities than the average continental crust. Also the wide-angle data revealed that the IRB is characterized by high velocities. This feature was then interpreted as sill-like structure built up by a series of mafic intrusions. Therefore, a key issue is to study if this relatively mafic crust is consistent with other geophysical observables. Based on the velocity models, two lithospheric density models have been derived along the IBERSEIS wide-angle transects. The geoid, gravity and topography response of these models have been calculated using a finite elements code that solves, simultaneously, the geopotential, lithostatic, and heat flow equations. The resulting values are then compared with the measured observables and the crustal and lithospheric mantle geometry and density is modified until the best fit is obtained. The initial density models calculated from the seismic data adjust quite well to the real potential field data. However, minor modifications have been required in order to properly fit the observables. The final density models are consistent with the existence of relatively high density bodies in the mid-crust providing further support to the seismic interpretation. In addition, they place new constraints on the location of the lithosphere–asthenosphere boundary and on the tectonic evolution of SW-Iberia.

1. Introduction

Integrated geophysical modelling has been used since the early 90s to investigate the depths and mechanisms of isostatic compensation in ocean plateaus and swells (Wessel, 1993; Gevemeyer, 1999). This integrated modelling analysis consists in forward modelling of as many geophysical observables as possible. These can include gravity, geoid, magnetic field, heat flow, etc. With these observables Earth's scientists have been able to constrain crustal thickness, continental

deformation in convergent orogens (Sandiford and Powell, 1990; Zhou and Sandiford, 1992; Petit et al., 2008), intraplate stress and associated deformation at different scales, from global to tectonic plate (Coblentz et al., 1994), and the lithospheric structure (Ebbing et al., 2006).

Zeyen and Fernàndez (1994) designed a powerful modelling approach that integrates gravity, elevation and heat flow under local isostatic equilibrium assumption to investigate the two-dimensional thermal and density structure of the lithosphere. These authors pointed out the need to have well constrained models of the crust by using seismic information. This approach was further improved incorporating the geoid elevation and has been successfully used to model the lithosphere in different scenarios as NE-Iberia (Zeyen and Fernàndez, 1994), the North Iberian Margin (Ayarza et al., 2004), the transition from the Variscan Belt to the Jurassic oceanic crust in SW-

* Corresponding author. Tel.: +34 93 4095410; fax: +34 93 4110012.
E-mail addresses: ipalomeras@ija.csic.es (I. Palomeras), rcarbo@ija.csic.es (R. Carbonell), puy@usal.es (P. Ayarza), mfernandez@ija.csic.es (M. Fernàndez), simancas@ugr.es (J.F. Simancas), djmp@ugr.es (D.M. Poyatos), lodeiro@ugr.es (F. González Lodeiro), andres@ija.csic.es (A. Pérez-Estaún).

Iberia (Fernàndez et al., 2004), the NW Moroccan margin and Atlas mountains (Zeyen et al., 2005; Teixell et al., 2005), and the Tibetan Plateau (Jiménez-Munt et al., 2008).

The SW-Iberian Peninsula constitutes part of the Iberian Massif and represents one of the best exposed fragments of the European Variscan basement (Fig. 1). It was produced by the oblique compression between three tectonic zones: the South Portuguese Zone (SPZ), the Ossa-Morena Zone (OMZ) and the Central Iberian Zone (CIZ). Since the early 90s this area has been the aim of numerous studies including surface geology (Fonseca and Ribeiro, 1993; Azor et al., 1994; Fonseca et al., 1999; Simancas et al., 2001; Azor et al., 2008), deep normal incidence seismic profiles (Simancas et al., 2003; Carbonell et al., 2004), magnetotelluric surveying (Monteiro-Santos et al., 1999; Almeida et al., 2001; Monteiro Santos et al., 2002; Pous et al., 2004; Muñoz et al., 2005; Almeida et al., 2005) and wide-angle seismic refraction profiling (Palomeras et al., 2009).

The active source vertical incidence seismic experiment IBERSEIS (Simancas et al., 2003; Carbonell et al., 2004) showed evidence of a high reflective body located at midcrustal levels within the OMZ and CIZ. High P-wave velocities found in this area after modelling coincident dense wide-angle seismic data suggested that this band of reflectivity most probably represents a mantle derived mafic intrusion located at 15–20 km depth (Palomeras et al., 2009). This high velocity body, identified in both wide-angle transects, is roughly coincident in shape and depth with the high amplitude reflectivity band identified by the normal incidence deep seismic reflection section as the Iberseis Reflective Body (IRB) (Simancas et al., 2003; Carbonell et al., 2004). The wide-angle seismic models featured typical lower crust velocities (up to 7 km/s) beneath the IRB. The Moho discontinuity is almost horizontal along the entire transect and located at 32–33 km depth. Palomeras et al. (2009) conclude that the crust in SW-Iberia is laterally variable and the modelled high velocities are consistent with the existence of mantle derived rocks. Seismic full waveform synthetic simulations done by Flecha et al. (2009) indicate that the high velocity areas can be modelled as small lenses randomly distributed with velocity variations of less than 0.2 km/s. These authors conclude that the high velocity areas, lower crust and Moho are not homogeneous but intruded by lenses of mafic material. Accordingly, all the seismic data sets indicate that the crust in the area is relatively mafic in composition. A key issue is whether or not this mafic crust is consistent with the response of other geophysical observables in the area. To resolve this, we have used an integrated modelling code that combines heat flow, gravity, geoid elevation and topography to obtain a lithospheric-scale model of SW-Iberia.

The modelling has been carried out along two, approximately 650-km long, profiles that run across the Gulf of Cadiz (GC) and the SW-Iberia Variscan Belt (Fig. 1). Both transects overlap the wide-angle seismic transects acquired in the area, crossing the three tectonic provinces (SPZ, OMZ and CIZ). A lithospheric model of SW-Iberia that fits the potential field observables and the seismic data is finally obtained. This model is regarded as the best constrained lithospheric section of SW-Iberia.

2. Methodology

In order to model the lithospheric structure in SW-Iberia, a combination of different geophysical observables is used. In this study, the seismic model has been used as constraint of the structure and initial density distribution within the crust: normal incidence seismic data gave us information about the crustal structure geometries, and the wide-angle data about the physical properties of the crust, i.e. P-wave velocities and density distribution calculated from the P-wave velocities.

To undertake modelling, the lithospheric section is divided into a number of bodies with different physical properties: thermal conductivity, radiogenic heat production, and density. The top of the model corresponds to Earth's surface and the bottom to the lithosphere–asthenosphere boundary (LAB). The densities for the crust were derived from the seismic velocities and are discussed in a specific section. The density of the lithospheric mantle is assumed to be temperature dependent (Parson and Sclater, 1977) according to

$$\rho_m = \rho_a(1 + \alpha(T_a - T(Z))), \tag{1}$$

where ρ_a is the density of the asthenosphere, α is the thermal expansion coefficient, and T_a is the temperature of the asthenosphere. Using a 2D finite element algorithm (Zeyen and Fernàndez, 1994) the steady state temperature distribution is calculated. The temperature at the surface and at the LAB is considered to be constant and equal to 15 °C and 1350 °C, respectively. After the temperature distribution has been determined, the density is evaluated at each node of the mesh and with this density distribution the gravity, geoid and topography anomalies are calculated using a finite elements code that solves simultaneously the geopotential, lithostatic and heat transport equation (CAGES) (Zeyen and Fernàndez, 1994). In
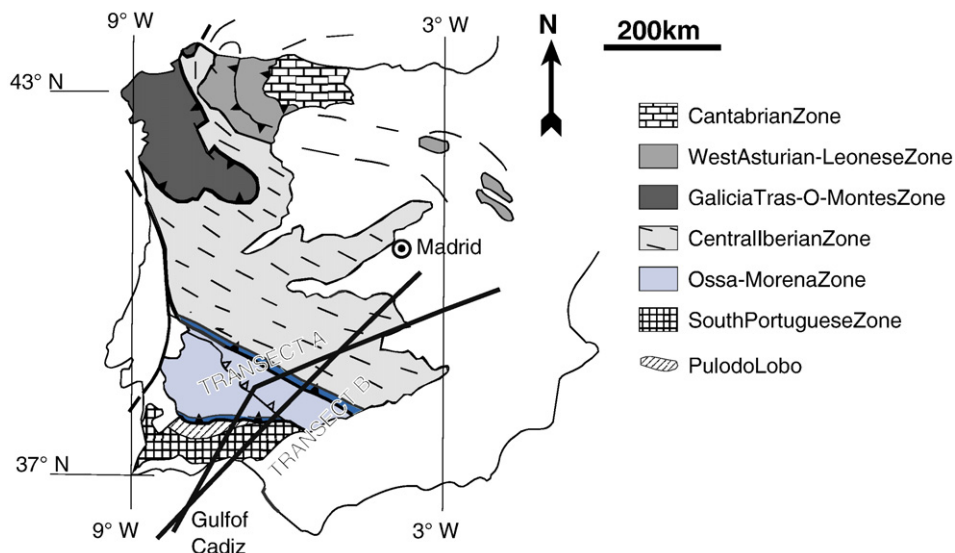

Fig. 1. Map of the main geological units and tectonic zones of the study area. Modelled transects are indicated by solid black lines.

particular, to calculate the topography, local isostatic equilibrium is assumed. Resulting values for the topography, Bouguer anomaly and geoid height are then compared with the observed ones, and the initial model is modified until the best fit is obtained. As a result, a lithospheric structure and its density and temperature distribution is obtained. The details of the formulation and the specifications of the modelling scheme have been published elsewhere (Zeyen and Fernàndez, 1994; Zeyen et al., 2005).

The Bouguer anomaly is calculated using Talwani's 2D algorithm (Talwani et al., 1959) for each triangle element of the mesh, thus allowing for density variations depending on pressure, temperature and lithology. The geoid height is calculated using an algorithm based on the solution of the gravity potential using Brun's formula for a rectangular prism which is formed by adjacent triangular elements and extends to infinity in a direction perpendicular to the strike of the lithospheric section (Zeyen et al., 2005). Elevation is calculated for every column of the mesh by comparing its buoyancy with that corresponding to the average mid-oceanic ridge column under the assumption of local isostasy and following Lachenbruch and Morgan (1990). The depth of isostatic compensation to calculate elevation,

and gravity and geoid anomalies is taken at the maximum depth reached by the lithospheric mantle along the transect, and the space between this depth and the base of the model is filled with asthenospheric material of constant density.

3. Observables

Data used in this study (Fig. 2) have been compiled from different sources. Topographic data was taken from the ETOPO2 Global database (Smith and Sadwell, 1994; Sandwell and Smith, 1997; Hastings and Dunbar, 1999). In the study area the elevation ranges between 500 and 700 m height in the north decreasing to a depth near 2400 m b.s.l. in the GC.

Geoid height data was taken from EGM96 (Lemoine et al., 1998). In order to avoid effects of sublithospheric density variations, the geoid signature corresponding to the spherical harmonics developed until degree and order 8 were removed. The geoid data reveals a maximum of 10 m just in the middle of our transects, decreasing to 5 m at the edges.
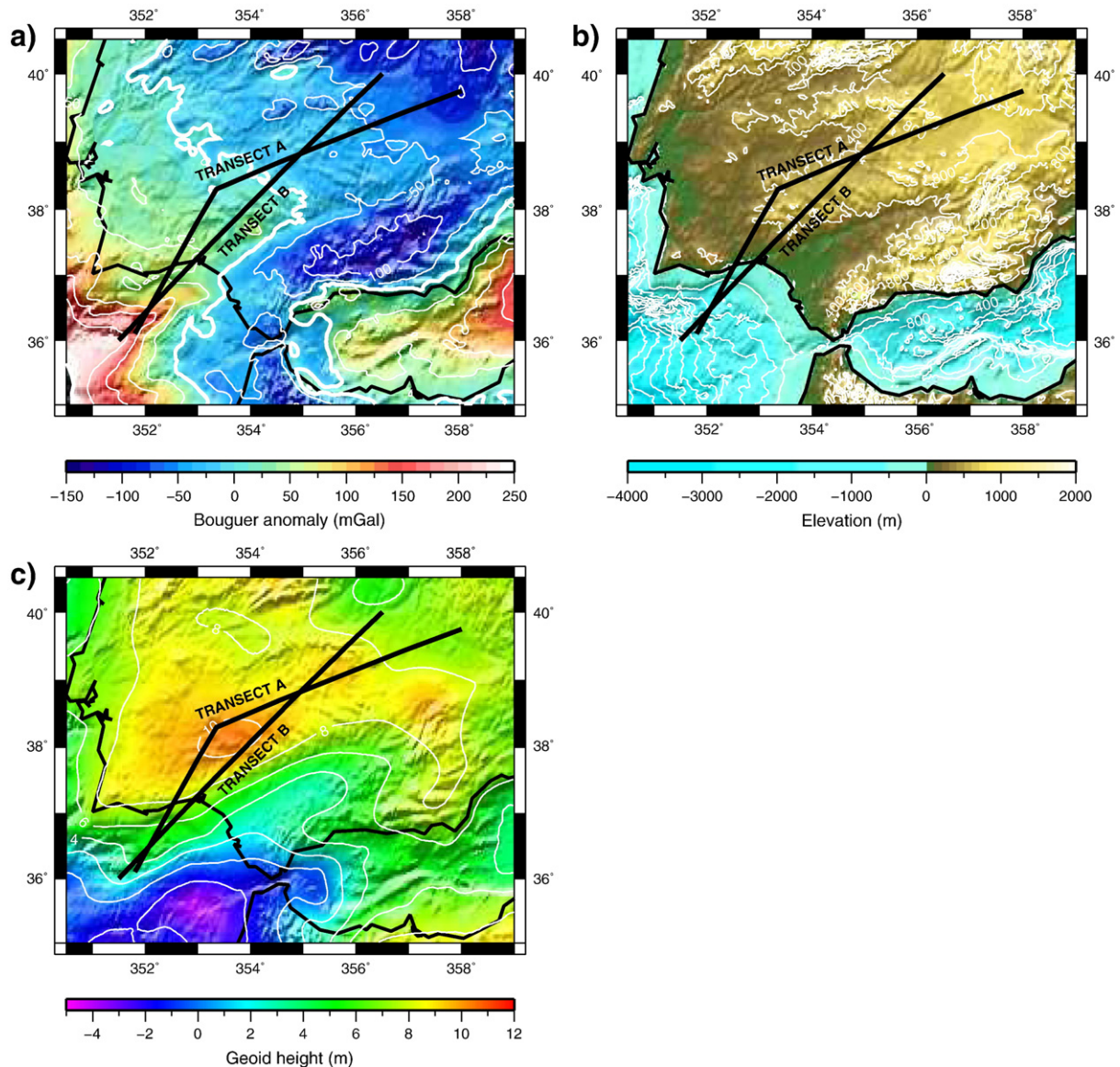
Fig. 2. Observables used for the study area. a) Bouguer anomaly (from Spanish Instituto Geografico Nacional (Mezcua et al., 1996) for the continental area and from (Fullea et al., 2008) for the oceanic area) The 0 mGal isoline is marked with a thick white line, b) Topography (from ETOPO2 Global database (Smith and Sadwell, 1994; Sandwell and Smith, 1997; Hastings and Dunbar, 1999)) and c) Geoid height (from EGM96 (Lemoine et al., 1998)). Solid black lines indicate the position of the transects modelled in this study.

Bouguer anomaly data for the continental area comes from the Spanish Instituto Geografico Nacional (IGN) database (Mezcua et al., 1996) and from Fullea et al. (2008) for the oceanic area. Gravity anomaly values decrease from 200 mGal at the southern edge of the models to negative values of less than −50 mGal at the northern edge of our profiles. The data show a prominent positive anomaly across the SPZ and OMZ which, considering that the Moho is almost flat, probably indicates an anomalous density distribution inside the crust. The 0 mGal isoline does not follow the coast line as is expected for a passive margin. The gravity, geoid and topography data along the transect were averaged every 2.5 km from a 25 km strip on both sides of the profile.

Heat flow data comes from Fernàndez et al. (1998) and Marzan (2000). These authors compiled heat flow and heat production data from water and mining exploration wells and oil wells, offshore and onshore. As a result they obtained the surface heat flow map of Iberia and its margins. In the SW, there are several samples for the SPZ and south of the OMZ, but there are no samples for the CIZ. Therefore, we only have heat flow values for the southern part of our transects. For each transect, heat flow values have been taken from the intersection of the transect with a heat flow isoline of the heat flow map of the Iberian Peninsula (Fernàndez et al., 1998), with a dispersion of ± 10 mW/m².

The heat flow values range from 50 mW/m² for the oceanic lithosphere to values higher than 70 mW/m² in the SPZ, decreasing to values near 60 mW/m² in the OMZ. North of the OMZ there is no available data but the isolines suggest that the heat flow could have values that range between 60 and 70 mW/m².

4. Modelling input data

This work aims to obtain two-dimensional lithospheric density models of SW-Iberia in order to test if the relatively mafic mid to lower crust obtained by the wide-angle experiment IBERSEIS-WA is consistent with the other geophysical observables: Bouguer anomaly, geoid height, heat flow and topography. The models we present coincide with the tracks of the wide-angle transects presented by Palomeras et al. (2009). In order to avoid border effects and to get enough penetration to model lithospheric mantle depths, the models extend a few hundred kilometres south and north at both ends of the wide-angle transects. Therefore, two lithospheric sections that run from the GC to the CIZ through the SW-Iberian Variscan Belt are modelled. Each lithospheric section is divided into bodies with different petrophysical properties: density, thermal conductivity and radiogenic heat production.

4.1. Densities

Density information is only available for the upper crust. However, because there is a relatively large number of well constrained seismic data based models, densities can be estimated from P-wave velocities. In this study the modelled sections coincide with the two P-wave seismic velocity models derived by Palomeras et al. (2009). These data was used to estimate the densities within the crust in the central part of the sections. To constrain the crustal densities to the south, into the GC, we used the interpreted seismic near-vertical reflection and refraction/wide-angle data (González-Fernández et al., 2001) acquired in the GC during the Iberian Atlantic Margins (IAM) project (Banda et al., 1995). To fix the crustal structure and densities to the north, the results from Suriñach and Vegas (1988) and Díaz et al. (1993) were used. The velocity models built by these data have been transformed into densities (Fig. 3) using the velocity–density relationship of Christensen and Mooney (1995) for the upper crust and Sobolev and Babeyko (1994) for the middle and lower crust.

Christensen and Mooney (1995) approach is only corrected for pressure, whereas Sobolev and Babeyko (1994) approach is corrected for pressure and temperature. Therefore, Christensen and Mooney (1995) approach is perhaps more appropriate for common upper crustal rocks which typically feature a more felsic composition, whereas Sobolev and Babeyko (1994) derived a scheme for anhydrous magmatic rocks, which are mostly more mafic. Thus, Sobolev and Babeyko (1994) relationship is usable for basic magmatic and crystalline rocks, typical of mid-to-lower crustal levels. Majdański et al. (2009) compared the influence of different density–Vp relations on density values recalculated from seismic velocities on geoid anomalies in Poland. These authors concluded that Sobolev and Babeyko (1994) relationship is the one that suits better for the lower crust. The resulting density distribution was used to divide the crust into bodies/domains characterized by a constant density (Fig. 3). For Transect A, the wide-angle data used in the central part (Palomeras et al., 2009) is not well constrained at the northern part. Therefore, the shape of the bodies in this area comes from the coincident normal incidence seismic image IBERSEIS (Simancas et al., 2003). Density values of these bodies were taken from Transect B, since it is only a few kilometres apart in this area.

The density models feature, for the shallow upper crust, densities that range from 2350 to 2450 kg/m^3 (body 2 in Fig. 3). These densities are consistent with a broad variety of rocks but they are lower than the expected for the outcropping rocks (granite and quartzites). It could be due to weathering and fracturing that affect these rocks at shallow depths. Therefore, densities reported for these rocks (Christensen and Mooney, 1995) were taken for body number 2 in the modelling. At upper crustal depths, densities vary within 2590–2690 kg/m^3 (bodies 3 and 4 in Fig. 3) which are consistent with granite and quartz monzonite. Beneath this level there are mainly two bodies with densities that range within 2750–2850 kg/m^3 (bodies 5 and 6 in Fig. 3) which could be represented by anorthosite, gabbros and felsic granulites. At this same level, denser units with densities of 2950–2980 kg/m^3 (bodies 7 and 9 in Fig. 3) are present. These bodies can be represented by rocks with a more mafic composition, as mafic granulites, diabase, garnet granulites, etc. The highly reflective-high velocity body identified in the seismic data corresponds to the body number 8 (Fig. 3) which features densities that approach values of 3000 kg/m^3. This implies rocks with a relatively high content in mafics. The lower crust features densities that reach values of 2950–2980 kg/m^3 (body 10, in Fig. 3). Rock types which can have these densities are gabro-norite, mafic granulites, diabase, etc. Both models contain bodies that are characterized by very high density in the mid-to-lower crust (bodies 7, 8 and 9 in Fig. 3).

4.2. Thermal conductivity

Studies of thermal conductivity are scarce in the area and only limited measures in wells within the OMZ are available (Fernàndez et al., 1998). An indirect method to get the thermal conductivity is to know the lithology. Nevertheless, there is no evident correlation between lithology and thermal conductivity. In the published data, there is a great variability of thermal conductivity values for each rock type due to data heterogeneity (mineral composition, porosity, saturation) and experimental conditions. In this study we used the data compiled by Clauser and Huenges (1995), where they obtained a range of thermal conductivity values for different rock types. In the study area, Palomeras et al. (2009) proposed a crustal column with possible crustal lithologies that where consistent with the seismic P-wave velocities. Taking into account these lithologies, the thermal conductivity for each body in the model was chosen within the range obtained by Clauser and Huenges (1995) and according to typical crustal values as in Fernàndez et al. (2004). The final values were refined by the best fit with the observables.

4.3. Radiogenic heat production

As with the thermal conductivity values, there is a great variability of radiogenic heat production values for each rock type. This depends
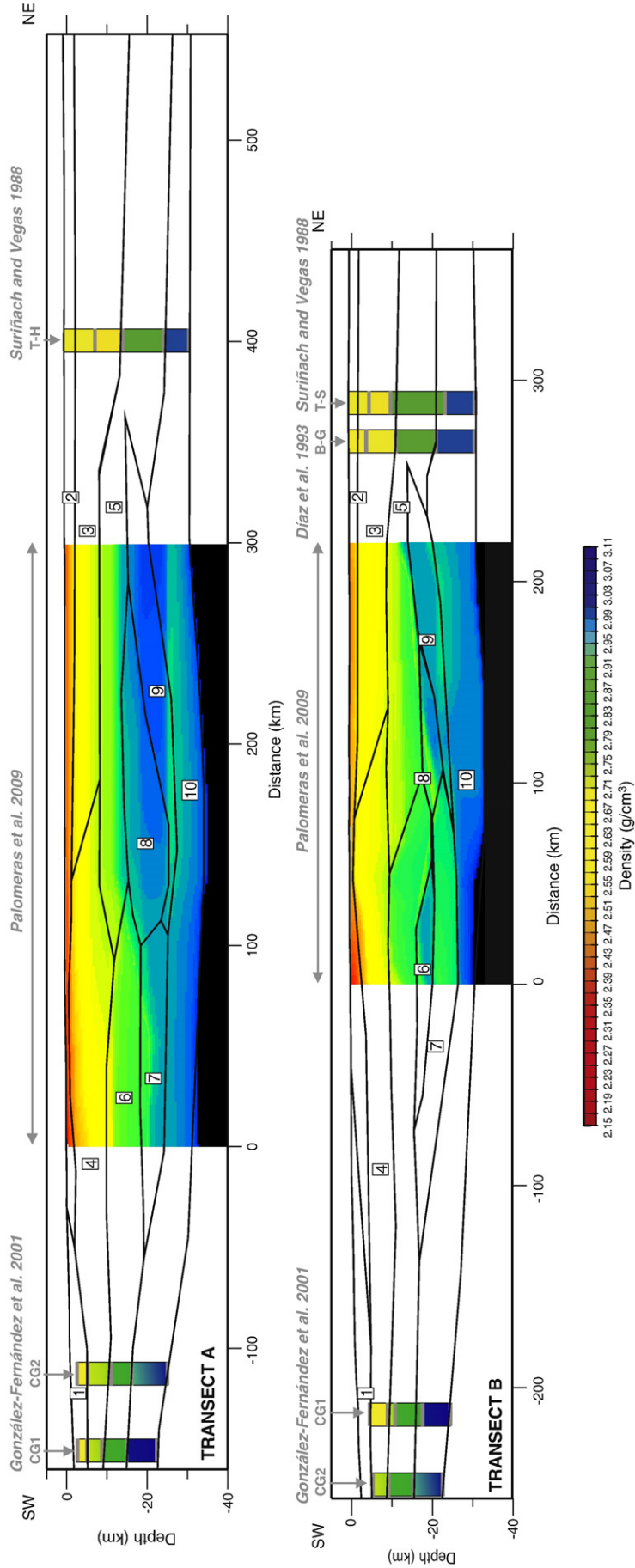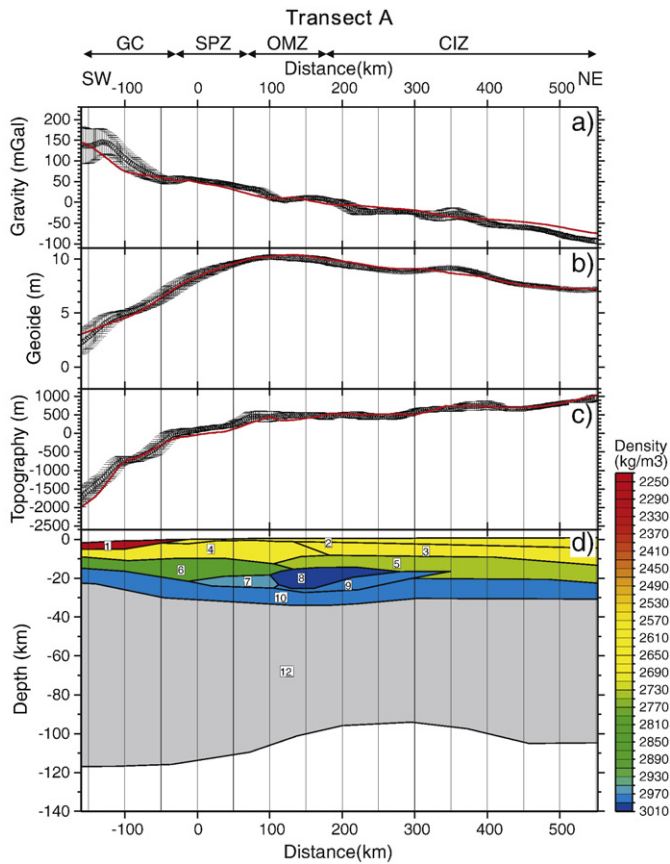
Fig. 3. Crustal structure of the study area inferred from seismic profiles data (see text for explanation). Geometry of these crustal bodies has been used as input in the modelling for Transect A (top panel) and Transect B (bottom panel).
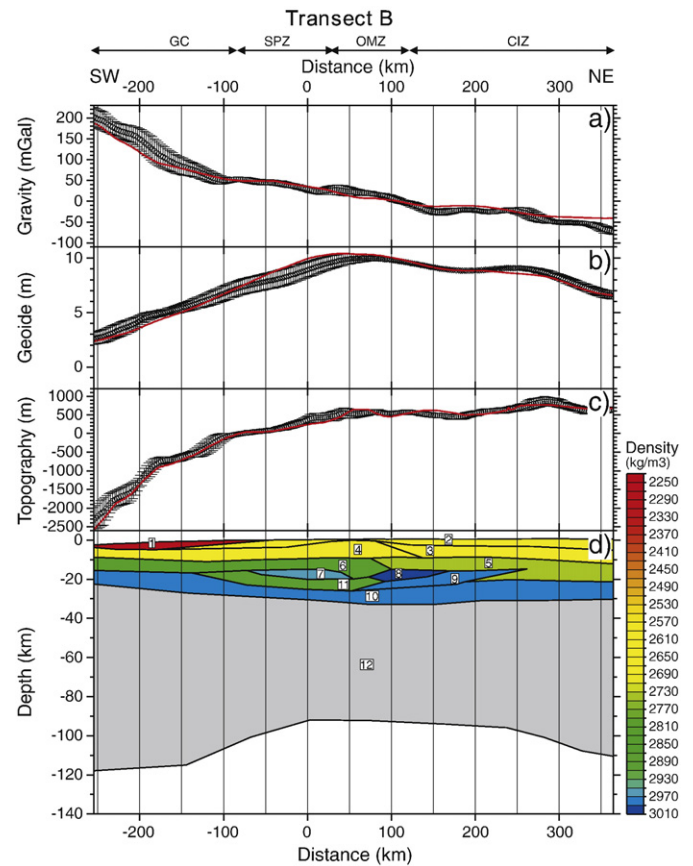
Fig. 4. Results along Transect A. a) Bouguer anomaly, b) geoid height and c) topography. The observed data is averaged with the values up to 25 km each side of the profile and is represented by dots with dispersion bars corresponding to the standard deviation within this range of 25 km at each side of the profile. Solid lines are the calculated values for the model shown in d).

Fig. 5. Results along Transect B. a) Bouguer anomaly, b) geoid height and c) topography. The observed data is averaged with the values up to 25 km each side of the profile and is represented by dots with dispersion bars corresponding to the standard deviation within this range of 25 km at each side of the profile. Solid lines are the calculated values for the model shown in d).

on how enriched in heat production elements the rock sample is. Fernàndez et al. (1998) calculated the radiogenic heat production in surface rock samples from the Iberian Massif and Betic orogenic belt. The values obtained in this work were used to define the heat production of the surface bodies within the Variscan Belt. Mafic rocks have low content in heat production elements (Rudnick and Fountain, 1995), then for the middle crust intrusions and lower crust, heat production values less than 0.5 μW/m^3 were chosen. For the rest of the bodies for which there are no heat production measurements, typical values were taken and adjusted with the observable data.

Upper mantle heat production is smaller than that of the crust. Accordingly, the mantle value used for the heat production was 0.01 μW/m^3, that is in the range obtained by Rudnick et al. (1998) for off-craton peridotites. Radiogenic heat production values were also adjusted with the surface heat flow measured.

5. Results

At the starting models, high density bodies were placed at middle and lower crustal levels, obtaining a reasonably good fit between the model and the observables. Further changes in the densities and body thickness were small and restricted within the uncertainty range of the P-wave velocities reported by Palomeras et al. (2009) and to the associated error in the Vp–density relationship (less than 70 kg/m^3 for the upper crust (Christensen and Mooney, 1995), and 10 kg/m^3 for the lower crust (Sobolev and Babeyko, 1994)). The crustal structure is well constrained by the seismic data, nevertheless we have more freedom in the lithospheric thickness. Consequently, we have mostly changed the depth of the LAB to fit the measured elevation, gravity

and geoid. Modelling of the complete lithosphere is difficult due to uncertainties underlying the models of the LAB. While its influence on the Bouguer gravity is not prominent, the one on the geoidal signal is higher. In the study area values concerning the depth of the LAB boundary are scarce. Fullea et al. (2007) modelled the lithospheric thickness using elevation, geoid anomaly and thermal data at the Gibraltar Arc System and adjacent zones with a 1D code. The LAB depth proposed by these authors was adopted in the initial models. Subsequent slight changes in the LAB geometry were needed in order to fit the observables.

Resulting models are shown in Figs. 4 and 5. The three graphs on top show the observed and calculated values of Bouguer anomaly, geoid height and topography for the lithospheric structure shown at the bottom. The observed data are taken every 2.5 km along the profile and they are averaged with the values up to 25 km each side of the profile. These averaged values are represented by dots with dispersion bars corresponding to the standard deviation within this range of 25 km to each side of the profile. Solid lines are the values calculated from the model. The resulting models are in good agreement with the observables.

According to the physical properties, the sections were divided into 11 different bodies (Table 1) with different properties. Density distribution in the transects shows differences in the crust of the southern part with respect to the north. In both transects the upper crust (from 0 to 10–12 km depth) can be divided into two parts: one within the GC, SPZ and OMZ (body number 4) and another less dense within the CIZ (body number 3). Beneath these levels, up to 15 km depth, the crust within the GC and the SPZ (body number 6) is denser than within OMZ and CIZ (body number 5). Below, at mid crustal

Table 1

Physical parameters of the different bodies used in the modelling transects. Lithospheric mantle density is temperature dependent: $\rho_m(z) = 3200(1-3.5 \times 10^{-5} \, ^{\circ}C^{-1}(T(z)-T_a))$.

Body Number	Description	Heat Production ($\mu W/m^3$)	Thermal Conductivity (W/m·K)	Density (kg/m^3)
1	Marine sediments	1.2	2.3	2250
2	Upper crust	2.0	2.5	2600
3	Upper crust OMZ-CIZ	2.5	2.5	2600
4	Upper crust GC-SPZ	3.0	2.5	2680
5	Middle crust OMZ-CIZ	2.0	2.0	2740
6	Middle crust GC-SPZ	2.0	2.0	2810
7	Intrusion SPZ	0.3	2.1	2950
8	Intrusion OMZ-CIZ (IRB)	0.3	2.5	2990
9	Intrusion OMZ-CIZ	0.3	2.1	2970
10	Lower crust	0.3	2.5	2980
11	Upper lower crust GC-OMZ Transect B	0.3	2.1	2880
12	Lithospheric Mantle	0.01	3.2	T-dependent

Fig. 6. Top panel shows the surface heat flow calculated (solid line) for the model on Transect A, compared with the measured values (dots), which are taken from the intersection of the profile with a heat flow isoline of the Iberian Peninsula heat flow map (Fernàndez et al., 1998). Bottom panel: Lithosphere temperature distribution predicted for the model.

levels, there are high density bodies (body numbers 7, 8 and 9) that correspond to the high velocity lenses in the velocity models from Palomeras et al. (2009). These bodies are smaller in the Transect B than in Transect A. Beneath the dense body within the SPZ in Transect B (body number 7) a less dense body is modelled (body number 11). At lower crustal levels there is no difference between the three tectonic provinces. The Moho discontinuity is almost flat and located at 32–33 km depth within the CIZ, OMZ and northern part of SPZ. The crust becomes thinner within the GC reaching depths of 25 km at the southern edge of the profiles. Resulting LAB is located at 120 km depth within the GC and it shallows to 95 km depth within the OMZ and southern part of CIZ. Then it thicks again at the northern edge of the profiles to 105–110 km depth. Both models are quite similar presenting the same bodies with small changes in geometry/shape. The most remarkable difference between both models is that in Transect B the high density bodies placed at mid crustal levels (body numbers 7, 8 and 9) are smaller and this transect features a lower density body (body number 11) beneath body number 7.

Resulting lithosphere temperature distribution and surface heat flow are shown in Figs. 6 and 7. Heat flow values of the area (upper panel Figs. 6 and 7) have been taken from the heat flow map of the Iberian Peninsula obtained by Fernàndez et al. (1998). Each observable value is the intersection of the profile with a heat flow isoline, with an average error of ±10 mW/m², as the authors report. Calculated heat flow is shown as a solid line and it follows the regional trend in the area.

The thermal regime shows a smooth distribution of typical passive margins, as is expected for the area.

## 6. Uncertainties and model resolution

Resulting models agree with the crustal structure and density distribution fixed with the seismic data. The main changes are in the northern part. The most important uncertainty is associated with the thermal conductivity and the radiogenic heat production. A slight change in one of these parameters yields a new temperature distribution that affects the mantle density, and to compensate the new mantle density, a change in the LAB topography is needed in order to fit the observed geoid elevation and topography, since the crustal structure is fixed by the seismic data.

A resolution test was carried out using the resulting density models obtained from the velocity models ±0.2 km/s, that is the maximum error associated to the velocity models obtained by Palomeras et al. (2009). This error in Vp corresponds to a difference in density of ~90 kg/m³, 10–20 kg/m³ bigger than the standard deviation of the Vp–density relationships used (Sobolev and Babeyko,
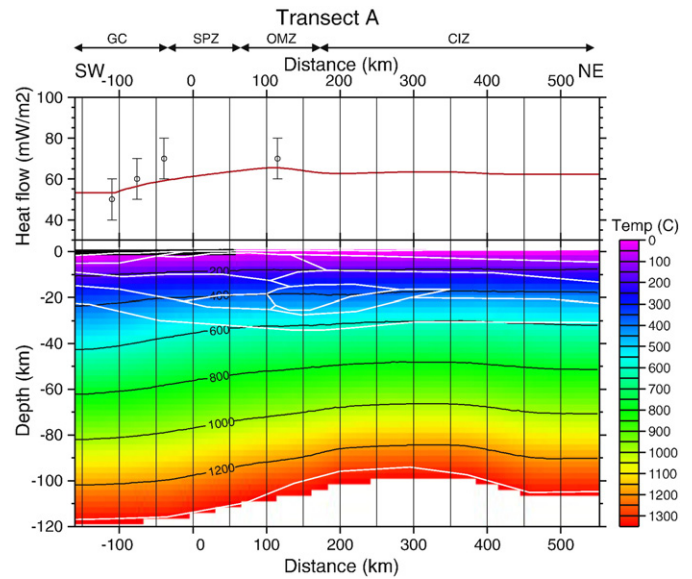
1994; Christensen and Mooney, 1995). With the new density values it was not possible to adjust the data with less error than the presented models. The best fit in the geopotential fields (Bouguer anomaly and geoid) and topography, without changes in the new densities, was obtained changing the LAB topography. The resulting models for the densities calculated with Vp + 0.2 km/s have an abrupt LAB topography, with the LAB depth being only 40 km within the OMZ and reaching 95 km depth at the southern edge. With this new model the heat flow is higher (more than 80 μW/m³), specially in the centre of the profile, being higher than the observed tendency. The resulting model for the densities calculated with Vp-0.2 km/s has a LAB almost
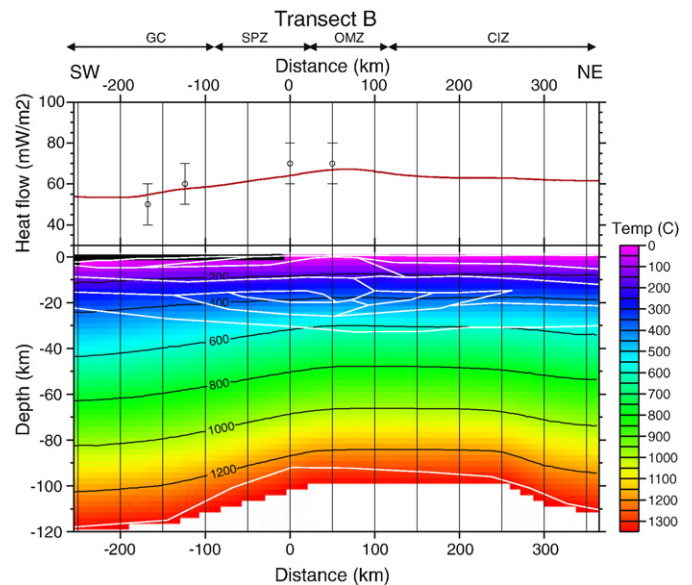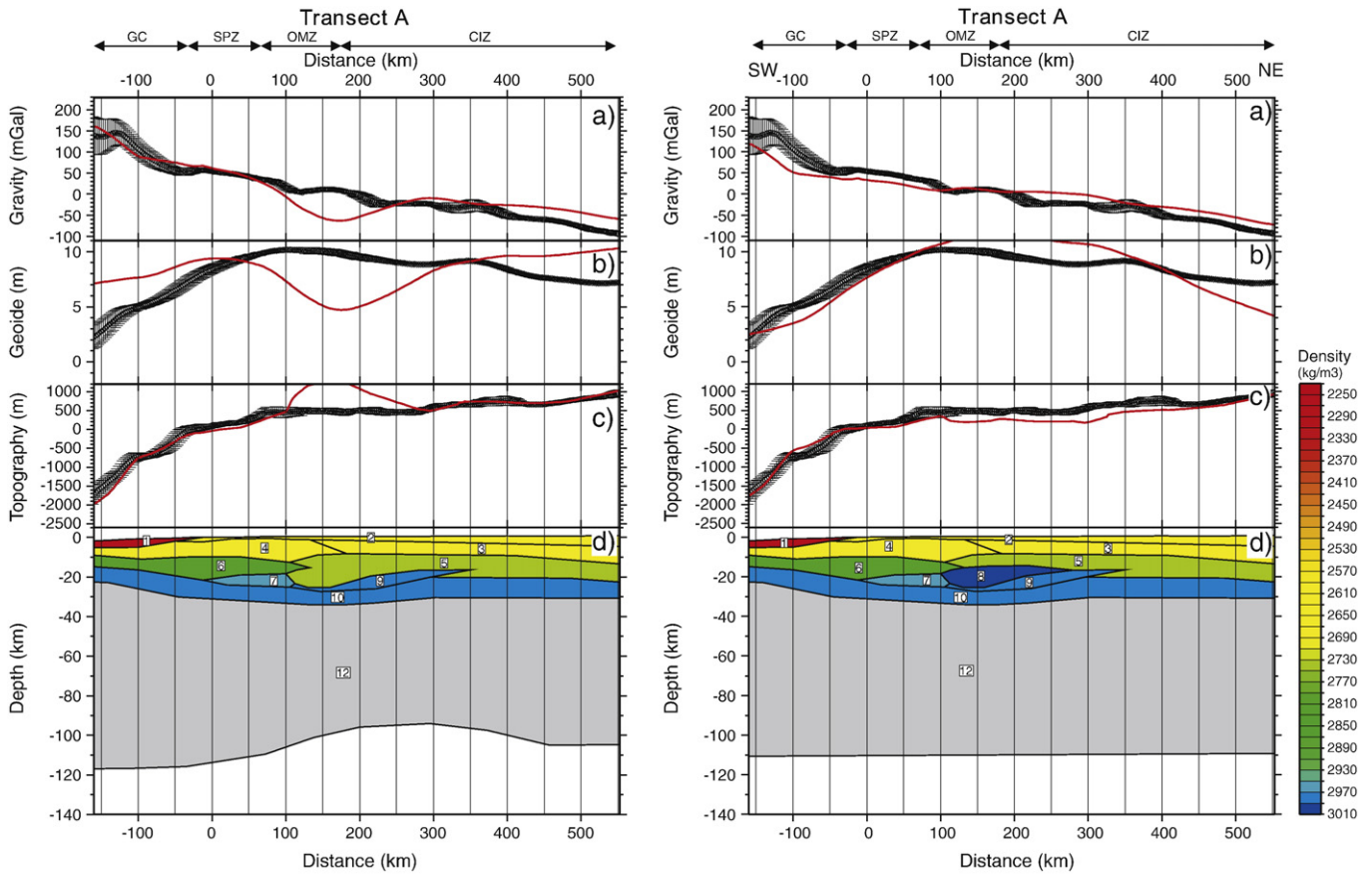

Fig. 7. Top panel show the surface heat flow calculated (solid line) for the model on Transect B, compared with the measured values (dots), which are taken from the intersection of the profile with a heat flow isoline of the Iberian Peninsula heat flow map (Fernàndez et al., 1998). Bottom panel: Lithosphere temperature distribution predicted for the model.

Fig. 8. Left panel: Transect A as presented in Fig. 4 without high density body number 8. It is seen that in order to fit the observables an increase in density between kms 100 and 250 is needed. Rigth panel: Transect A as presented in Fig. 4 with a flat LAB. Crustal structure is constrained by the seismic data, therefore in order to fit the observables an uplift in the LAB topography is needed. a) Bouguer anomaly, b) geoide data, c) topography, and d) model for the calculated values represented as a solid line in a), b) and c).

flat at 140 km depth being 10 km deeper within the OMZ. In this model the heat flow is 30 μW/m^3, lower than the measured one.

In order to prove the sensitivity of the data to the density variations in the middle crust, we removed the body number 8 in Transect A (Fig. 8). This body is small but is in the regional scale (big compared to the crustal thickness), therefore it has a signature in the observable data as is shown in the figure. It is seen that in order to match the data an increase in density within the crust from kilometres 100 to 300 is necessary. This test point out that the resulting values are sensitive to the relatively small body number 8. In order to prove how the datasets are sensitive to changes in the LAB topography we flattened the LAB (Fig. 8). The LAB topography is reflected in the geoid data. Since the crustal structure is constrained by the seismic data, in order to fit the data, especially the geoid data, a thinning of the lithosphere (upwelling the LAB topography) is required.

7. Discussion

This work aims to present a lithospheric model of SW-Iberia that integrates different geophysical observables with the results provided by the seismic dataset. These observables are mostly governed by the temperature and density distributions in the crust and lithospheric mantle, which are strongly dependent on the composition/nature of the lithosphere itself. An important goal of this work is to validate the crustal structure and physical properties obtained by seismic data. This, in turn, would provide some new insights on the possible geometry of the LAB.

A simple model for the crust was achieved dividing it into different domains and/or bodies with homogeneous physical properties: density, thermal conductivity, and heat production. Densities are

relatively well constrained by the seismic P-waves velocities, but there is little knowledge on the thermal conductivity and heat production. Therefore, a theoretical model was built that was consistent with the available observables. In this modelling approach the thermal conductivity has been considered isotropic in order to avoid complexities and due to the lack of detailed data. In reality, thermal conductivity of many rocks is strongly anisotropic. In addition, it is broadly known that values measured in laboratory deviate from the in-situ measurements even when environmental conditions are take into account. Thermal conductivity can also be estimated from the mineralogical composition and content. However, for the same rock type, the mineral content can vary from one sample to another. Therefore, the thermal conductivity for a single rock type may range between values that differ a factor greater than 2 (Clauser and Huenges, 1995).

The resulting model is well constrained down to Moho depths: the density model derived from the seismic velocities using Christensen and Mooney (1995) and Sobolev and Babeyko (1994) generate potential fields which match the tendency measured for both transects. The modelling benefits from a well constraint location for the Moho in the central part of the section (Simancas et al., 2003; Carbonell et al., 2004; Palomeras et al., 2009) and agrees with an almost flat, horizontal crust-mantle transition, located at 32–33 km depth. However the modelling exercise developed in this manuscript extends the constraints on the Moho laterally to the SW, into the GC and towards the NE beneath the central part of the Iberian Peninsula. High density bodies are required in order to be able to reproduce the measurements of the potential field data. Nevertheless, they are located in different parts in both sections and have different sizes, being bigger in Transect A.

Previous studies by Marzan (2000) concluded with a model which featured an important increase in thickness of the middle crust versus the upper crust towards the north in order to account for the gravity signature. In our models (Figs. 4 and 5) the gravity anomaly increase is accounted by using higher densities at the mid crustal levels. Therefore the multidisciplinary modelling (Figs. 4 and 5) is consistent with the existence of a relatively high density and high velocity material underlying the OMZ and CIZ which can be interpreted as a mafic layer, and/or mafic sill as proposed by Simancas et al. (2003); Carbonell et al. (2004); Flecha et al. (2009) and Palomeras et al. (2009).

In this modelling, the lithospheric mantle density is assumed to be temperature dependent. This is a realistic assumption, however, it introduces additional complexity and uncertainty in the modelling calculations. The temperature dependence implies that a slight change in the thermal conductivity of the bodies yields a new steady state of the temperature distribution in the model. This new physical state results in a new lithospheric mantle density distribution. These changes in the mantle density will directly influence the geoid anomalies and the surface topography. Therefore, in order to adapt the new calculated observables to the measured observations a change in the geometry of the LAB is required. The LAB is not constrained by seismics and the only knowledge available about its position in this area comes from similar modelling studies by Fullea et al. (2007). Although the observations and published measurements related to heat flow in SW-Iberia are relatively scarce, the modelling results shown in Figs. 4 and 5 place some physically reasonable constraints on the position and geometry of the LAB. A relatively small thinning (15–20 km) of the lithosphere is required to fit the geoid elevation and it is present in both transects. This thinning is located within the OMZ and the southern part of the CIZ (from km 150 to km 400 in Transect A and from km 0 to km 250 in Transect B). Large scale seismic experiments such as the ILIHA constrained the lithosphere up to depths larger than 100 km. Díaz et al. (1996) did an analysis of the ILIHA seismic data, a DSS experiment carried out in the Iberian Peninsula in the late 80s, and proposed an interpretation in which the base of the lithosphere was deeper than 90 km. The data also revealed evidence for anisotropy within the upper mantle. In our models the LAB is located at a depth of 120 beneath the GC, it shallows to 95 km in the northern SPZ and the OMZ, and thickens again towards the northern end of the transects, beneath the Central Iberian Plateau (Meseta).

Some of the characteristic features of the lithospheric and crustal structure of these models can be interpreted as a snapshot of the interaction between a mantle plume and the lithosphere in SW-Iberia during the Early Carboniferous. Since the early 80s a lot of vivid discussions on the consequences of plume–lithosphere interactions have been published (Anderson, 1982, 1998; Kukkonen and Peltonen, 1999; Sleep, 2003a,b; King, 2005), a large majority of them centred in the Archean. Nevertheless, evidences for plume activity exist at all geological ages. In particular, the abundant emplacement of dikes and sills during the Carboniferous and Early Permian in the Variscan Europe (Benek et al., 1996; Wilson et al., 2000; Ledru, 2000) has been interpreted as igneous activity related to intensive plume–lithosphere interaction. However, there is not a general agreement on the results of plume–lithosphere interactions. Modelling studies (for example, Burov et al. (2007), among others) suggest that this interaction can cause: crustal and lithospheric thinning, relatively large scale doming (topographic uplift), igneous activity, etc. These features can be responsible for significant gravity and geoid anomalies, and increase in the heat flow. The interactions between plumes and the lithosphere have also important consequences for tectonic and mineralogical evolution. The presence of the plume-head at relatively shallow levels can cause that deep material can rise to the surface rapidly (Fe + Mg rich magmas) (Sleep, 2003a,b; Nyblade and Sleep, 2003). Thus the plumes will trigger heating and melting of the lower crust and mantle

lithosphere (Saleeby et al., 2003). These features described by different authors can be observed in the area: for example the mineralization studies by Casquet et al. (2001); Tornos and Casquet (2005) and Tornos (2006), support the existence of magmas at mid crustal levels. These needed to be placed there by a high heat flow anomaly which could be the result of the head of the plume beneath the OMZ. This plume activity resulted also in the present lithospheric structure characterized by a relatively large amount of mafic material intruded at mid crustal levels and moderate lithospheric thinning inherited from the times when the plume was active. This lithospheric thinning happens to be the key of the present day isostatic equilibrium in the OMZ and CIZ. The plume also might have caused local domal uplift that resulted in extension, especially towards the northern part of the study area (CIZ) were normal faults and extensional basins of Carboniferous age are observed jointly with limited amount of volcanics.

8. Conclusions

A multidisciplinary geophysical modelling study is carried out in SW-Iberia in order to test the validity of wide-angle derived velocity models and to shed some light on the lithospheric structure of an area affected by the Variscan deformation. The point of departure are two 650 km long crustal sections divided in blocks with densities calculated from wide-angle velocities and thermal conductivity and heat production taken from measurements done in the area. The potential field response and the topography of these sections are then calculated and the sections are modified until there is a good fit between observed and modelled values.

Observed Bouguer anomaly values require of a dense middle crust in the OMZ and the CIZ, in agreement with the results of the wide-angle models. Accordingly, the lithosphere has to be thinned from 115 km to 95 km in the areas where these dense rocks are found in order to fit the topography and the geoid elevation data and to get isostatically equilibrated.

The high velocity dense rocks located at mid crustal depths are interpreted as sill-like bodies intruded during the Early Carboniferous plume activity and extension that affected SW-Iberia. In addition, shallowing of the lithosphere–asthenosphere boundary is viewed as remnants of the lithospheric thinning related to the stage of plume activity. Although the lithosphere was probably thinned in the Carboniferous to less than the 95 km observed today, the cooling of the area and subsequent transpression modified the position of the LAB to the point where isostatic equilibrium was reached.

Acknowledgements

References

Almeida, E., Monteiro Santos, F., Mateus, A., Heise, W., Pous, J., 2005. Magnetotelluric measurements in SW Iberia: new data for the Variscan crustal structures. Geophys. Res. Lett. 32 (8), 1–4.
Almeida, E., Pous, J., Santos, M., Fonseca, P., Marcuello, A., Queralt, P., Nolasco, R., Mendes-Victor, L., 2001. Electromagnetic imaging of a transpressional tectonics in SW Iberia. Geophys. Res. Lett. 28 (3), 439–442.
Anderson, D., 1982. Hotspots, polar wander, Mesozoic convection and the geoid. Nature 297, 391–393.
Anderson, D.L., 1998. The scales of mantle convection. Tectonophysics 284 (1–2), 1–17.
Ayarza, P., Martínez-Catalán, J., Alvarez-Marrón, J., Zeyen, H., Juhlin, C., 2004. Geophysical constraints on the deep structure of a limited ocean–continent subduction zone at the North Iberian Margin. Tectonics 23, TC1010.

Azor, A., González-Lodeiro, F., Simancas, J., 1994. Tectonic evolution of the boundary between the Central Iberian and Ossa-Morena zones (Variscan Belt, Southwest Spain). Tectonics 13, 45–61.

Azor, A., Rubatto, D., Simancas, J., González-Lodeiro, F., Martínez-Poyatos, D., Martín-Parra, L., Matas, J., 2008. Reic Ocean ophiolitic remnants in southern iberia questioned by SHRIMP U–Pb zircon ages of Beja-Acebuches amphibolites. Tectonics 27, TC5006.

Banda, E., Torné, M., the Iberian Margins Group, 1995. Iberian Atlantic Margins Group investigates deep structure of ocean margins. Eos. Trans. AGU 76 (3), 25,28-29.

Benek, R., Kramer, W., McCann, T., Scheck, M., Negendank, J.F.W., Korich, D., Huebscher, H.D., Bayer, U., 1996. Permo-Carboniferous magmatism of the Northeast German Basin. Tectonophysics 266, 379–404.

Burov, E., Guillou-Frottier, L., d'Acremont, E., Pourhiet, L.L., Cloetingh, S., 2007. Plume head–lithosphere interactions near intra-continental plate boundaries. Tectonophysics 434 (1–4), 15–38.

Carbonell, R., Simancas, F., Juhlin, C., Pous, J., Pérez-Estaún, A., González-Lodeiro, F., Muñoz, G., Heise, W., Ayarza, P., 2004. Geophysical evidence of a mantle derived intrusion in SW Iberia. Geophys. Res. Lett. 31 (11), 1–4 L11601.

Casquet, C., Galindo, C., Tornos, F., Velasco, F., Canales, A., 2001. The Aguablanca Cu–Ni ore deposit (Extremadura, Spain), a case of synorogenic orthomagmatic mineralization: age and isotope composition of magmas (Sr, Nd) and ore (S). Ore Geol. Rev. 18, 237–242.

Christensen, N., Mooney, W., 1995. Seismic velocity structure and composition of the continental crust: a global view. J. Geophys. Res. 100 (B6), 9761–9788.

Clauser, C., Huenges, E., 1995. Rocks Physics and Phase Relations. A Handbook of Physical Constants. AGU Reference Shelf Series, Ch. Thermal Conductivity of Rocks and Minerals, Vol. 3, pp. 105–126.

Coblentz, D., Richardson, R., Sandiford, M., 1994. On the gravitational potential of the earth's lithosphera. Tectonics 13 (4), 929–945.

Díaz, J., Gallart, J., Córdoba, D., Senos, L., Matias, L., Suriñach, E., Hirn, A., Maguire, P., 1993. A deep seismic sounding investigation of lithospheric heterogeneity and anisotropy beneath the Iberian Peninsula. Tectonophysics 221 (1), 35–51.

Díaz, J., Hirn, A., Gallart, J., Abalos, B., 1996. Upper-mantle anisotropy in SW Iberia from long-range seismic profiles and teleseismic shear-wave data. Phys. Earth Planet. Inter. 95 (3–4), 153–166 dynamics of the Subcontinental Mantle: From Seismic Anisotropy to Mountain Building.

Ebbing, J., Braitenberg, C., Götze, H.-J., 2006. The lithospheric density structure of the Eastern Alps. Tectonophysics 414 (1–4), 145–155.

Fernàndez, M., Marzán, I., Correia, A., Ramalho, E., 1998. Heat flow, heat production, and lithospheric thermal regime in the Iberian Peninsula. Tectonophysics 291 (1–4), 29–53 Jun.

Fernàndez, M., Marzán, I., Torne, M., 2004. Lithospheric transition from the Variscan Iberian Massif to the Jurassic oceanic crust of the Central Atlantic. Tectonophysics 386 (1–2), 97–115 Jul.

Flecha, I., Palomeras, I., Carbonell, R., Simancas, F., Ayarza, P., Matas, J., González-Lodeiro, F., Peréz-Estaún, A., 2009. Seismic imaging and modelling of the lithosphere of SW-Iberia. Tectonophysics 472 (1–4), 148–157.

Fonseca, P., Munhá, J., Rosas, F., Moita, P., Araujo, A., Leal, N., 1999. Variscan ophiolites and high-pressure metamorphism in southern Iberia. Ofioliti 24, 259–268.

Fonseca, P., Ribeiro, A., 1993. Tectonics of the Beja-Acebuches ophiolite: a major suture in the Iberian Variscan Foldbelt. Geol. Rundsch. 82, 440–447.

Fullea, J., Fernàndez, M., Zeyen, H., 2008. FA2BOUG-A FORTRAN 90 code to compute Bouguer gravity anomalies from gridded free-air anomalies: application to the Atlantic–Mediterranean transition zone. Comput. Geosci. 34 (12), 1665–1681.

Fullea, J., Fernàndez, M., Zeyen, H., Vergés, J., 2007. A rapid method to map the crustal and lithospheric thickness using elevation, geoid anomaly and thermal analysis. Application to the Gibraltar Arc System and adjacent zones. Tectonophysics 430 (1–4), 97–117.

Gevemeyer, I., 1999. Isostatic geoid anomalies over mid-plate swells in the Central North Altantic. Geodynamics 28 (1), 41–45.

González-Fernández, A., Córdoba, D., Matias, L., Torné, M., 2001. Seismic crustal structure in the Gulf of Cadiz (SW Iberian Peninsula). Mar. Geophys. Res. 22, 207–223.

Hastings, D.A., Dunbar, P.K., 1999. Global land one-kilometer base elevation (GLOBE) digital elevation model, documentation, 1st Edition. Key to Geophysical Records Documentation (KGRD), Volume 1.0, p. 34.

Jiménez-Munt, I., Fernàndez, M., Vergés, J., Platt, J.P., 2008. Lithosphere structure underneath the tibetan plateau inferred from elevation, gravity, and geoid anomalies. Earth Planet. Sci. Lett. 267, 276–289.

King, S.D., 2005. Archean cratons and mantle dynamics. Earth Planet. Sci. Lett. 234 (1–2), 1–14.

Kukkonen, I.T., Peltonen, P., 1999. Xenolith-controlled geotherm for the central Fennoscandian Shield: implications for lithosphere–asthenosphere relations. Tectonophysics 304 (4), 301–315.

Lachenbruch, A., Morgan, P., 1990. Continental extension, magmatism and elevation; formal relations and rules to thumb. Tectonophysics 174, 39–62.

Ledru, P., 2000. 305 Ma crustal-scale hydrothermal paleofield in the French Massif Central (western Variscides). April Geoscience2000 Conference. Manchester University.

Lemoine, F., Smith, D., Kunz, L., Smith, R., Pavlis, E., Pavlis, N., Klisko, S., Chinn, D., Torrence, M., Williamson, R., Cox, C., Rachlin, K., Wang, Y., Kenyon, S., Salman, R., Trimmer, R., Rapp, R., Nerem, R., 1998. Gravity, Geoid, and Marine Geodesy. The development of the NASA GSFC and NIMA joint geopotential model. Springer-Verlag, Berlin, Ch, pp. 461–469.

Majdański, M., Kozlovskaya, E., Świeckak, M., Grad, M., 2009. Interpretation of geoid anomalies in the contact zone between the East European Craton and the Palaeozoic Platform—I. Estimation of effects of density inhomogeneities in the crust on geoid undulations. Geophys. J. Int. 177, 321–333.

Marzan, I., 2000. Régimen Térmico en la Península Ibérica. Estructura Litosférica a través del Macizo Ibérico y el Margen Surportugués. Ph.D. thesis, Univ. Barcelona, Barcelona, Spain.

Mezcua, J., Gil, A., Benarroch, R., 1996. Estudio gravimétrico de la Península Ibérica y Baleares. Instituto Geográfico Nacional, Madrid.

Monteiro Santos, F., Mateus, A., Almeida, E., Pous, J., Mendes-Victor, L., 2002. Are some of the deep crustal conductive features found in SW Iberia caused by graphite? Earth Planet. Sci. Lett. 201 (2), 353–367.

Monteiro-Santos, F., Pous, J., Almeida, E., Queralt, P., Marcuello, A., Matias, H., Mendes-Victor, L., 1999. Electrical conductivity of the crust across the Ossa Morena and South Portuguese Zone suture. Tectonophysics 313, 449–462.

Muñoz, G., Heise, W., Paz, C., Almeida, E., Santos, F., Pous, J., 2005. New magnetotelluric data through the boundary between the Ossa Morena and Centroiberian Zones. Geol. Acta 3 (3), 215–223.

Nyblade, A.A., Sleep, N., 2003. Long lasting epeirogenic uplift from mantle plumes and the origin of the Southern African Plateau. Geochem. Geophys. Geosyst. 4.

Palomeras, I., Carbonell, R., Flecha, I., Simancas, F., Ayarza, P., Matas, J., Martínez Poyatos, D., Azor, A., González-Lodeiro, F., Pérez-Estaún, A., 2009. The nature of the lithosphere across the Variscan Orogen of SW-Iberia: Dense wide-angle seismic reflection data. J. Geophys. Res. 114.

Parson, B., Sclater, J., 1977. An analysis of the variations of ocean floor bathymetry and heat flow with age. J. Geophys. Res. 82, 803–827.

Petit, C., Tiberi, C., Deschamps, A., Déverchére, A., 2008. Teleseismic traveltimes, topography and the lithospheric structure across central Mongolia. Geophys. Res. Lett. 35, L11301.

Pous, J., Muñoz, G., Heise, W., Melgarejo, J., Quesada, C., 2004. Electromagnetic imaging of Variscan crustal structures in SW Iberia: the role of interconnected graphite. Earth Planet. Sci. Lett. 217 (3–4), 435–450.

Rudnick, R., Fountain, D., 1995. Nature and composition of the continental crust: a lower crustal prespective. Rev. Geophys. 33 (3).

Rudnick, R., McDonough, W., O'Connell, R., 1998. Thermal structure, thickness and composition of continental lithosphere. Chem. Geol. 145 (3–4).

Saleeby, J., Ducea, M., Clemens-Knott, D., 2003. Production and loss of high-density batholithic root, southern Sierra Nevada. Tectonics. 22.

Sandiford, M., Powell, R., 1990. Some isostatic and thermal consequences of the vertical strain geometry in convergent orogens. Earth Planet. Sci. Lett. 98, 154–165 May.

Sandwell, D., Smith, W., 1997. Marine gravity anomalies from GEOSAT and ERS-1 satellite altimetry. J. Geophys. Res. 102, 10039–10054.

Simancas, F., Carbonell, R., González-Lodeiro, F., Estaún, A.P., Juhlin, C., Ayarza, P., Kashubin, A., Azor, A., Poyatos, D.M., Almodóvar, G., Pascual, E., Sáez, R., Expósito, I., 2003. Crustal structure of the transpressional Variscan orogen of SW Iberia: SW Iberia deep seismic reflection profile (IBERSEIS). Tectonics 22 (6), 1062.

Simancas, F., Poyatos, D.M., Expósito, I., Azor, A., González-Lodeiro, F., 2001. The structure of a major suture zone in the SW Iberian Massif: the Ossa-Morena/Central Iberian contact. Tectonophysics 332 (1–2), 295–308.

Sleep, N.H., 2003a. Geodynamic implications of xenoliths gotherms. Geochem. Geophys. Geosyst. 4.

Sleep, N.H., 2003b. Survival of Archean cratonal lithosphere. J. Geophys. Res. 108.

Smith, W., Sadwell, D., 1994. Bathymetry prediction from dense satellite altimetry and sparse shipborne batrymetry. J. Geophys. Res. 99, 21803–21824.

Sobolev, S., Babeyko, A., 1994. Modeling of mineralogical composition, density and elastic wave velocities in anhydrous magmatic rocks. Surv. Geophys. 15, 515–544.

Suriñach, E., Vegas, R., 1988. Lateral inhomogeneities of the Hercynian crust in central Spain. Phys. Earth Planet. Inter. 51, 226–234.

Talwani, M., Worzel, J., Landisman, L., 1959. Rapid computations for two-dimensional bodies with application to the Mendocino submarine fracture zone. J. Geophys. Res. 64, 49–59.

Teixell, A., Ayarza, P., Zeyen, H., Fernández, M., M.L., A., 2005. Effects of mantle upwelling in a compressional setting: the Atlas Mountains of Morocco. Terra Nova 17, 456–461.

Tornos, F., 2006. Environment of formation and styles of volcanogenic massive sulfides: the Iberian Pyrite Belt. Ore Geol. Rev. 28 (3), 259–307.

Tornos, F., Casquet, C., 2005. A new scenario for related IOCG and Ni-(Cu) mineralization: the relationship with giant mid-crustal mafic sills, Variscan Iberian Massif. Terra Nova 17 (3), 236–241.

Wessel, P., 1993. Observational constraints on models of the Hawaiian hot spot swell. J. Geophys. Res. 98 (B9) 16095-16004.

Wilson, M., Timmerman, M., Network, P., 2000. Permo-Carboniferous magmatism in western and central Europe: plume impact versus plume incubation models. April Geoscience2000 Conference. Manchester University.

Zeyen, H., Ayarza, P., Fernàndez, M., Rimi, A., 2005. Lithospheric structure under the wester African-European plate boundary: a transect across the Atlas Mountains and the Gulf of Cadiz. Tectonics 24, TC2001.

Zeyen, H., Fernàndez, M., 1994. Integrated lithospheric modeling combining thermal, gravity, and local isostacy analysis: application to the NE Spanish Geotransect. J. Geophys. Res. 99, 18089–18102.

Zhou, S., Sandiford, M., 1992. On the stability of isostatically compensated mountain belts. J. Geophys. Res. 97 (B10), 14207–14221.